Proceedings of the 30th International Cosmic Ray Conference
Rogelio Caballero, Juan Carlos D'Olivo, Gustavo Medina-Tanco,
Lukas Nellen, Federico A. Sánchez, José F. Valdés-Galicia (eds.)
Universidad Nacional Autónoma de México,
Mexico City, Mexico, 2008

Vol. 2 (OG part 1), pages 513–516

30TH INTERNATIONAL COSMIC RAY CONFERENCE

ICRC'07 Mérida, México

An All-Sky Search for Intermediate-Scale Structure Using Milagro

G. P. WALKER[1] FOR THE MILAGRO COLLABORATION
[1]*Los Alamos National Laboratory, Los Alamos, NM*
gwalker@lanl.gov

Abstract: Milagro is a TeV gamma-ray observatory with a $\sim$ 2 sr field of view and a $> 90\%$ duty factor. The large field of view and long observation time make Milagro ideal for surveying large regions of the Northern Hemisphere sky. A previous all-sky survey searched for point sources [1], but the analysis is easily adaptable to look for intermediate-scale sources ($\sim 10^\circ$) as well. A search on intermediate scales has been conducted, and 2 unexpected regions of excess are seen with a statistical significance above 11σ. The results of some simple diagnostics to determine the nature of these excesses are discussed.

The Milagro Detector

Milagro [1] is a water-Cherenkov detector at an altitude of 2650m capable of continuously monitoring the overhead sky. It is composed of a central 60m x 80m pond with a sparse 200m x 200m array of 175 "outrigger" tanks surrounding it. The pond is instrumented with two layers of photomultiplier tubes. The top "air-shower" layer consists of 450 PMTs under 1.4m of purified water, while the bottom "muon" layer has 273 PMTs located 6m below the surface. The air-shower layer allows the accurate measurement of shower particle arrival times used for direction reconstruction and triggering. The greater depth of the muon layer is used to detect penetrating muons and hadrons to help distinguish between gamma-ray- and hadron-induced air showers. The outrigger array improves the angular resolution of the detector by providing a more accurate core location and a longer lever arm with which to reconstruct the events.

Milagro's large field of view ($\sim$ 2sr) and high duty cycle ($> 90\%$) allow it to scan the entire overhead sky continuously, making it well-suited for searching for new sources of TeV gamma rays, as well as monitoring known sources at higher energies. Previous surveys [1, 2] were optimized for sources smaller than Milagro's $\sim 1.1^\circ$ angular resolution. However, the analysis can easily be modified to search for larger sources.

Analysis Method

In the analysis, a signal map is made based on the arrival direction of each event. A background map is also created using a technique called "direct integration" [1], in which a two-hour time interval is used to generate the background. The accuracy of the background map depends on the assumption that the shape of the local cosmic ray flux is constant during the two hours. Since this time interval corresponds to the earth rotating 30°, this analysis is relatively insensitive to features with an extent larger than $\sim 30^\circ$ in Right Ascension.

In the standard analysis, the signal and background maps are smoothed with a bin size that is optimal for Milagro's angular resolution (PSF smoothing may be used instead), and then the maps are compared. In this analysis, however, a square bin of size 10° in Declination and $10^\circ/cos(\delta)$ in Right Ascension is used to increase the sensitivity to larger features. Because a 2-hour (30° in R.A.) background generation interval is used, a bin size larger than 10° is not feasible, especially at higher declinations. The analysis was applied to 6.5 years of data, beginning in July 2000 and ending in January 2007.

Preliminary Results

The top half of Figure 1 shows a preliminary all-sky map generated using 10° binning with no gamma/hadron cut applied. The bottom map was optimized for gamma-ray point sources and is included for comparison. While the Crab Nebula (at RA $= 83.6^\circ$, Dec $= 22.0^\circ$) is seen at 15σ in the bottom map, the significance at the Crab's location is only 4.7σ in the top map. This decrease is due to the large bin size as well as the lack of a gamma/hadron cut. The Cygnus Region (at RA $\approx 305^\circ$, Dec $\approx 40^\circ$), which was discussed in [3], is clearly visible in both maps. The regions of excess in the top map at RA $\approx 70^\circ$, Dec $\approx 15^\circ$, labeled "RegionA", and at RA $\approx 125^\circ$, labeled "Region B" both have peak significances above 11σ. This is above 9.5σ after accounting for the trials of searching the map and is clearly not due to statistical fluctuations. Systematic effects such as seasonal variation and year-to-year detector variation have been excluded as possible causes. In addition, the possibility of an underestimation of the background in these regions has been considered, but these features are found to be due to an excess in the signal map. Finally, if Universal Time (Solar Time) or anti-Sidereal Time are used, Regions A and B are not seen.

Note that both regions are paralleled by regions of deep deficit. This is because the background estimate has been contaminated (raised) by the large excesses. The effect of each excess extends out to $\pm 30^\circ$ in RA because of the 2-hour background generation interval.

Discussion

Region A is similar to an excess seen in results published by the Tibet ASγ Collaboration [4], which they labelled the "tail-in" anisotropy, and it is coincident with the direction opposite to the relative motion of the solar system with respect to the neutral gas [5]. Region B is not readily visible in the Tibet results. It is also noteworthy that this analysis is not suitable for features broader than $\sim 30^\circ$, such as the deficit in the Tibet maps. This deficit is also seen by Milagro, but with a different analysis [6].

The source of these features is not clear, but simple diagnostics have provided insight into the nature of Region A (Region B is still under investigation). If a cut of nTop > 150 is applied (nTop is the number of PMTs hit in the top layer), the significance of Region A drops only slightly from $\sim 15\ \sigma$ to $\sim 13\ \sigma$. However, based on the reduced number of events, the significance should have dropped to $\sim 7\ \sigma$ if Region A had the same nTop distribution as the background. If a gamma/hadron cut of A4 > 1 is used [3], the excess in Region A drops to $\sim 7\ \sigma$, which is only slightly higher than the $\sim 4\ \sigma$ that would be expected based on the reduction of statistics.

Figure 2 shows simulated nTop and A4 distributions for gamma rays and protons [7]. The -2.75 proton distribution in both plots approximates the measured cosmic-ray background distribution. In the nTop plot, gamma rays and protons with the same spectra are seen to have similar nTop distributions, and the distribution is seen to flatten as the spectrum hardens. Due to the observed strength of Region A when the nTop > 150 cut is used, the excess, whether it is due to gamma rays or hadrons, must have a spectrum harder than -2.75. However, as is seen in the A4 plot, gamma rays with a spectrum harder than -2.75 would have a significantly flatter A4 distribution than the background, so that if the excess were due to gamma rays, the significance would have increased when the A4 cut was applied. Thus, the large drop in significance observed with the A4 cut is inconsistent with gamma rays. Hard-spectrum protons, on the other hand, have an A4 distribution that is only slightly flatter than the background and are thus consistent with these observations.

These simple diagnostics show that the excess in Region A is strongly inconsistent with gamma rays as well as with the normal cosmic ray background. Instead, the excess is consistent with protons with a spectrum harder than -2.75. More complete diagnostics are underway to determine the spectrum of Region A more precisely, and also to determine the nature of Region B.

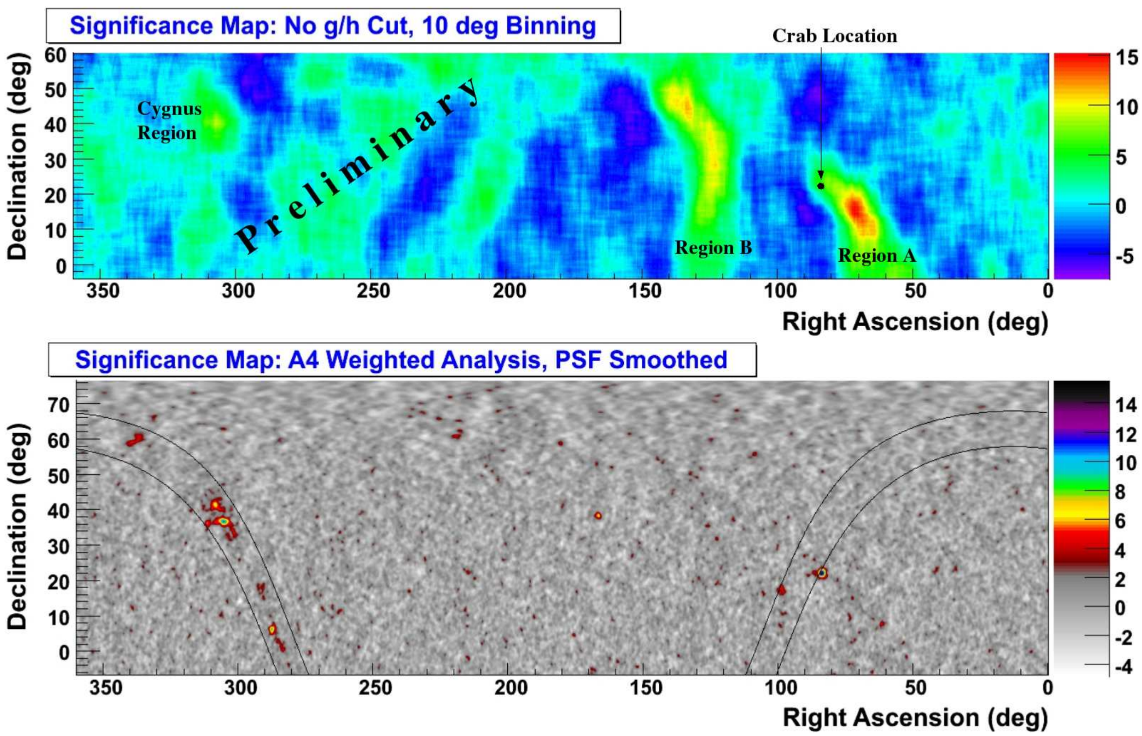

Figure 1: The top map is a preliminary all-sky significance map made with 10° binning and no gamma/hadron cut. The map is cut off above Dec$=\ 60^\circ$ because the width of the signal bin begins to approach the two-hour width (30°) of the background generation interval. The bottom map was optimized for gamma-ray point sources and is included for comparison. The black curves outline the Galactic Plane (at $b = \pm 5^\circ$).

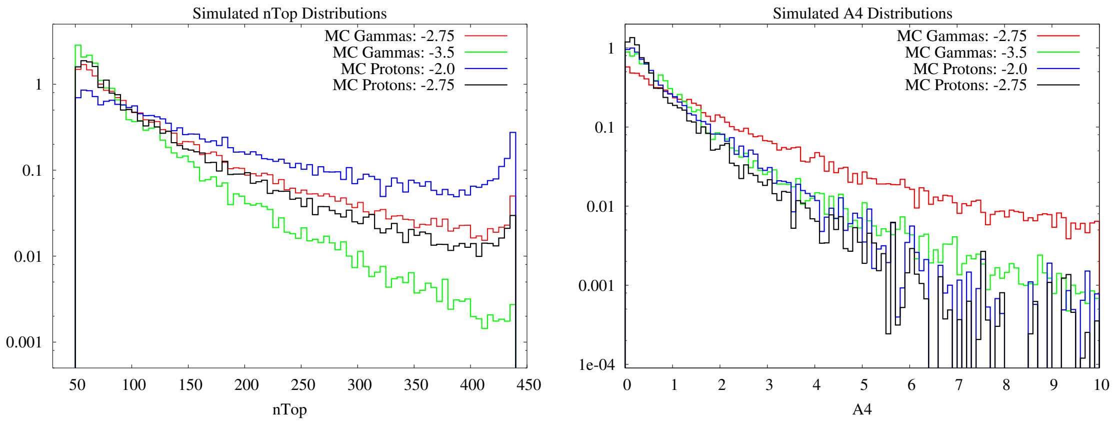

Figure 2: Distributions of nTop, which is the number of PMTs hit in the top layer, and A4, which is a gamma/hadron discriminator, for simulated gammas rays and protons with spectra as indicated in the plots. The nTop distributions for gamma rays and protons of the same spectral index are similar, while the distribution flattens for harder spectra. The strength of Region A when the nTop > 150 cut is used provides strong evidence that the spectrum of the excess is harder than -2.75. However, the A4 plot shows that hard-spectrum gamma rays should have increased in significance when the A4 > 1 cut was used. Instead, since the A4 distribution is seen to flatten slightly for hard-spectrum protons, the excess is consistent with protons that have a spectrum harder than -2.75.

Acknowledgements

We acknowledge Scott Delay and Michael Schneider for their dedicated efforts in the construction and maintenance of the Milagro experiment. This work has been supported by the National Science Foundation (under grants PHY-0245234, -0302000, -0400424, -0504201, -0601080, and ATM-0002744) the US Department of Energy (Office of High-Energy Physics and Office of Nuclear Physics), Los Alamos National Laboratory, the University of California, and the Institute of Geophysics and Planetary Physics.

References

[1] R. W. Atkins, et al., Tev gamma-ray survey of the northern hemisphere sky using the milagro observatory, Astrophys. J. 608 (2004) 680–685.

[2] A. A. Abdo, et al., Tev gamma-ray sources from a survey of the galactic plane with milagro, Astrophys. J. Lett. 664 (2007) L91–L94.

[3] A. A. Abdo, Detection of tev gamma-ray emission from the cygnus region of the galaxy with milagro using a new background rejection technique, AIP Conf. Proc. 867 (2006) 199–208.

[4] M. Amenomori, Anisotropy and corotation of galactic cosmic rays, Science 314 (2006) 439–443.

[5] K. Nagashima, K. Fujimoto, R. M. Jacklyn, Galactic and heliotail-in anisotropies of cosmic rays as the origin of sidereal daily variation in the energy region $< 10^4$ gev, Journal of Geophysical Research 103 (1998) 17429–17440.

[6] B. E. Kolterman, et al., A harmonic analysis of the large scale cosmic ray anisotropy, 30th ICRC, Merida, Mexico.

[7] V. Vasileiou, et al., Monte carlo simulation of the milagro gamma-ray observatory, 30th ICRC, Merida, Mexico.